JACS
JOURNAL OF THE AMERICAN CHEMICAL SOCIETY

Communication

pubs.acs.org/JACS

Coordination-Network-Based Ionic Plastic Crystal for Anhydrous Proton Conductivity

Satoshi Horike,*[,†,‡] Daiki Umeyama,[†] Munehiro Inukai,[§] Tomoya Itakura,[∥] and Susumu Kitagawa*[,†,§,⊥]

[†]Department of Synthetic Chemistry and Biological Chemistry, Graduate School of Engineering, Kyoto University, Katsura, Nishikyo-ku, Kyoto 615-8510, Japan

[‡]PRESTO, Japan Science and Technology Agency, 4-1-8 Honcho, Kawaguchi, Saitama 332-0012, Japan

[§]Institute for Integrated Cell-Material Sciences (WPI-iCeMS), Kyoto University, Yoshida, Sakyo-ku, Kyoto 606-8501, Japan

[∥]DENSO Corporation, 1-1 Showa-cho, Kariya, Aichi 448-8661, Japan

[⊥]ERATO Kitagawa Integrated Pores Project, Japan Science and Technology Agency, Kyoto Research Park Building #3, Shi-mogyo-ku, Kyoto 600-8815, Japan

Supporting Information

ABSTRACT: An ionic coordination network consisting of protonated imidazole and anionic one-dimensional chains of Zn^{2+} phosphate was synthesized. The compound possesses highly mobile ions in the crystal lattice and behaves as an ionic plastic crystal. The dynamic behavior provides a proton conductivity of 2.6×10^{-4} S cm^{-1} at 130 °C without humidity.

The design of highly mobile ions in crystalline solids has been a challenge because ions tend to be closely embedded in crystals with strong interactions. Meanwhile, ion-conductive solids are in high demand for applications such as battery electrolytes and molecular sensing. Among various ion conductors, plastic crystals are a unique class of compounds.[1] The term "plastic crystal" describes a compound that has a long-range-ordered crystal structure but short-range disorder, and several ion conductors such as lithium and proton have been reported.[2] Conventional plastic crystals are categorized as either molecular crystals or ionic crystals, and both categories of compounds are generally composed of "discrete" molecules or ions. Although ionic plastic crystals are promising as solid ion conductors, the strategy for their synthesis is limited because we should choose a discrete cation and anion having weak Coulombic interaction, and a new material platform is urgently required.

On the other hand, there are reports on the unusual dynamics of guest molecules absorbed in a new family of crystalline porous materials known as porous coordination polymers (PCPs) or metal−organic frameworks (MOFs), which consist of metal ions and organic linkers.[3] Some porous structures strongly enhance the mobility of adsorbed guests, and high proton conductivity is induced without water support.[4] In these cases, guests are accommodated as the neutral form in a disordered fashion and are not categorized as ionic plastic crystals. However, the internal spaces of coordination networks could create an ionic crystal structure with local plasticity and consequent ion conductivity. There have been many studies on materials with high proton conductivities at operating temperatures above 100 °C under anhydrous conditions,[5] and in this work we tried to create a new class of ionic plastic crystal based on an extended coordination network [a coordination-network-based ionic plastic crystal (CIPC)] and to elucidate its unique structure plasticity and proton-hopping mechanism.

The room-temperature reaction of ZnO with imidazole (ImH) and phosphoric acid (H_3PO_4) gave a white powder, sample **1**. To characterize its structure, we prepared a single crystal of **1** on which an X-ray diffraction (XRD) measurement was conducted at −30 °C. As shown in Figure 1, **1** has the formula $[Zn(HPO_4)(H_2PO_4)_2](ImH_2)_2$. The coordination networks are composed of tetrahedrally coordinated Zn^{2+} ions and two types of orthophosphates, and they form extended one-dimensional (1D) chain networks along the *a*

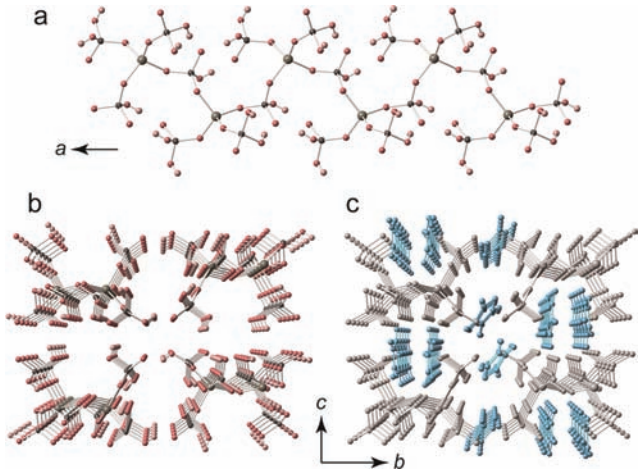

Figure 1. (a) Crystal structure of negatively charged 1D coordination chains of $[Zn(HPO_4)(H_2PO_4)_2]^{2-}$ in **1** and (b) packing structure of four 1D chains along the *a* axis. Zn, P, O, and H atoms are gray, black, red, and pink, respectively. (c) Crystal structure of **1**. The ImH_2^+ ions are highlighted in blue and the networks are gray. H atoms in the networks have been omitted.

Received: February 25, 2012
Published: April 18, 2012

dx.doi.org/10.1021/ja301875x | J. Am. Chem. Soc. 2012, 134, 7612−7615

axis. The 1D networks contain $[Zn(HPO_4)(H_2PO_4)_2]$ units possessing a charge of −2 (Figure 1a,b). The locations of the protons in the orthophosphates were confirmed by the bond distances of the P and O atoms. The P−OH distances range from 1.55 to 1.57 Å, and the P═O distances are 1.50−1.51 Å. The crystal structure shows that the unit formula contains one HPO_4^{2-} and two $H_2PO_4^-$ as ligands. For charge compensation, the two crystallographically independent imidazole molecules are both protonated and located in spaces between the 1D chains (Figure 1c), forming an ionic crystal system. There are multiple hydrogen bonds between protonated imidazole (ImH_2^+) ions and orthophosphates. The ImH_2^+ and orthophosphates in **1** were also characterized by IR and solid-state NMR studies. The IR spectrum showed peaks at 2500−3300 cm^{-1}, which are assigned to the N−H stretching of ImH_2^+ and higher wavenumbers of ImH. The solid-state ^{31}P NMR spectrum of **1** at 25 °C under static conditions had both broad and sharp Q_0 peaks. This suggests that different environmental orthophosphates exist in **1**.

The observed ImH_2^+ ions are packed close to each other, and it is possible to have interionic proton hopping with support of the negative Zn chains. There have been several reports of crystal structures containing anionic metal phosphate networks and protonated organic molecules, but in most cases these are robust 2D or 3D structures, and no studies of structure plasticity have been presented to the best of our knowledge.[6] The thermogravimetric analysis (TGA) profile of **1** shows no clear weight loss below 200 °C and a gradual decrease in weight above 200 °C. The decrease is probably the partial condensation of orthophosphate to pyrophosphate. The powder XRD patterns of **1** at 25 and 140 °C do not differ, indicating that the unit cell of the crystal structure is almost unchanged in this temperature range. On the basis of the structural characteristics, we investigated the ion conductivity of **1** by impedance spectroscopy from 25 to 130 °C under anhydrous conditions (Figure 2a). At 25 °C, the ion conductivity of **1** was 3.3×10^{-8} S cm^{-1}, and as temperature increased, we observed a jump in conductivity at around 55 °C, which then reached 2.6×10^{-4} S cm^{-1} at 130 °C. The conductivity was almost constant when the sample was kept for 12 h at 130 °C. Because the temperature-dependent XRD data showed that the crystal structure does not change in this temperature region, the observed conductivity behavior must be caused by local motion of the proton carrier ImH_2^+ in **1**. The nonlinear increase in conductivity at 55 °C suggests that the motion of mobile ions suddenly changed, which is a characteristic behavior of plastic crystals. As shown in Figure 3a, the differential scanning calorimetry (DSC) profile of **1** from 25 to 100 °C has a clear endothermic peak at 70 °C, which is slightly higher than 55 °C. The difference in these temperatures is due to the different rates of temperature increase for impedance and DSC measurements. Plastic crystals are defined as compounds that undergo a large-enthalpy-change phase transition from a solid phase to another solid phase, and in the case of molecular ionic plastic crystals, they then melt with an entropy change of <20 J mol^{-1} K^{-1}.[1a] For **1**, the entropy change at 70 °C from DSC is 6.6 J mol^{-1} K^{-1}, which is in the range of the criterion and one of the lowest values reported for ionic plastic crystals.

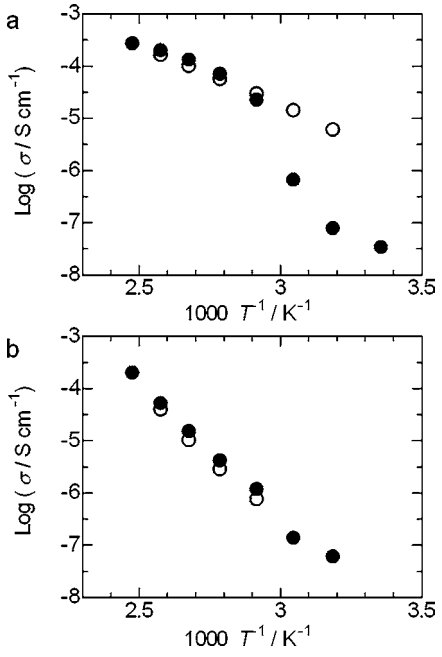

Figure 2. Arrhenius plots of anhydrous conductivity of (a) **1** from 25 to 130 °C (black) and 130 to 40 °C (white) and (b) **1**″ from 40 to 130 °C (black) and 130 to 70 °C (white).

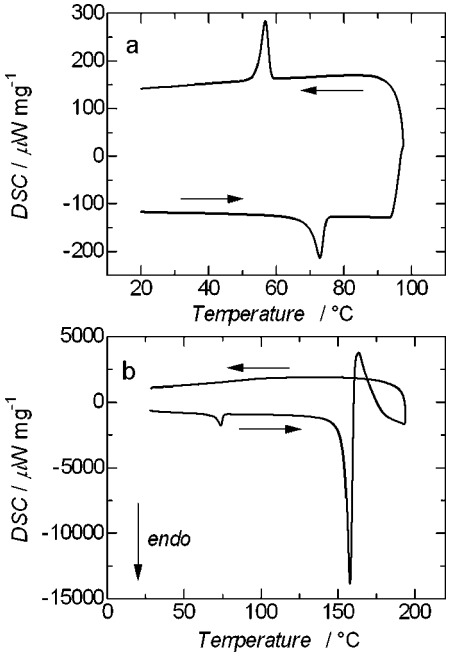

Figure 3. DSC curves of **1** from (a) 25 to 100 °C and (b) 25 to 200 °C.

For direct observation of the thermal activation of **1**, the single-crystal structure at 75 °C was studied (Figure 4b). In contrast to the structure at −30 °C (Figure 4a), one type of ImH_2^+ is heavily disordered in the plane of the five-membered ring, whereas the other ImH_2^+ is unchanged. This indicates a clear difference in mobility of ImH_2^+ below and above the endothermic change temperature (70 °C). The cell volumes of the crystal structures at −30 and 75 °C are almost identical, and the thermal factors of the Zn phosphate chains do not increase more than those of ImH_2^+. The increase in mobility of ImH_2^+ was also determined by variable-temperature solid-state ^2H NMR spectroscopy. The powder patterns of ^2H NMR analysis of deuterated **1**, which was synthesized using imidazole-d_4, from

dx.doi.org/10.1021/ja301875x | J. Am. Chem. Soc. 2012, 134, 7612−7615

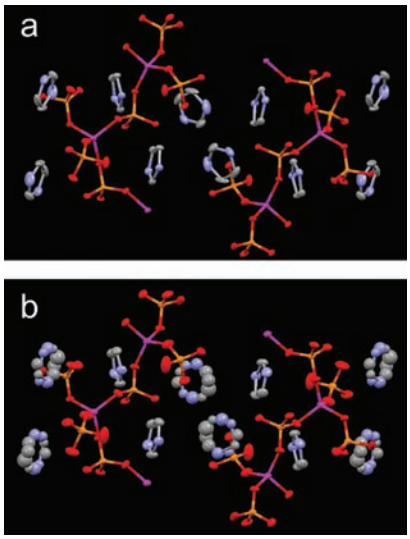

Figure 4. Partial crystal structures of **1** at (a) −30 °C and (b) 75 °C. Atoms represent thermal factors. Zn, P, O, N, and C atoms are purple, orange, red, blue, and gray, respectively. H atoms have been omitted.

25 to 130 °C clearly suggest that partial ImD_2^+ ions start to become more isotropic as the temperature increases. Solid-state static ^{31}P NMR analysis at 100 °C also suggests that the isotropy of the phosphate ligands increases and supports proton hopping. On the other hand, the conductivity from 130 to 40 °C (Figure 2a) shows a linear profile, resulting in the observation of hysteresis, while DSC showed an exothermic peak at 50 °C (Figure 3a). The linear profile of the Arrhenius plot can be explained by the supercooling behavior of ImH_2^+ in **1**. The calculated activation energy between 130 and 40 °C is 0.47 eV, and Grotthuss mechanisms mainly seem to contribute.[7] There has been no report on plastic crystals consisting of protonated imidazole (ImH_2^+) because of the large Coulombic interaction. The Zn coordination networks in **1** provide a delocalized anionic backbone for gentle entrapment of ImH_2^+ to produce fast motion in the solid.

It is important to assign the direct-current (DC) conductivity and conductive ion species to protons or other species. We fabricated a membrane-electrode assembly, and the electromotive force of the H_2/air cell was measured. The measurement showed an open-circuit voltage (OCV) of about 0.75 V at 150 °C without humidity, and the OCV was constant for 1 h without significant decay. This result suggests DC conductivity by protons in **1**, because oxide anion (O^{2-}) is not generated in the structure. As a result, we discovered that the proton-conductive plastic crystal consists of an ionic coordination network and that the supposed conduction mechanism is derived from the local dynamic motion of protonated imidazole (ImH_2^+). An acceleration of the dynamics of ImH_2^+ at around 70 °C promotes **1** to another crystalline phase having local plasticity.

Interestingly, the DSC curve of **1** from 25 to 200 °C (Figure 3b) shows endothermic peaks not only at 70 °C but also at 160 °C, although no weight loss was observed until 200 °C from the TGA study. This is a melting point of **1**, and the melted sample was highly viscous and transparent. In other words, the plastic phase of **1** ranges from 70 to 160 °C. The DSC curve from 200 to 25 °C does not have any clear peak, which indicates that no phase transition occurs in this temperature range. The melted **1** (denoted as **1′**) was cooled to room temperature, and powder XRD measurements showed no diffraction. **1′** is regarded as a metastable state of **1**, and the ionic components ImH_2^+ and Zn phosphates would retain a large disorder. We scratched **1′** to form a sample as a fine powder (denoted as **1″**) and checked the powder XRD at room temperature. The observed powder pattern is the same as for **1**, which is the original crystalline phase. This suggests that the recrystallization of amorphous **1′** to crystalline **1″** occurs by physical stimulus and that the chemical bonding and composition in **1** are intact during the overall transformations. Although the XRD pattern of **1″** is similar to that of **1**, the DSC curve of **1″** does not show an endothermic peak at 70 °C. The conductivity of **1″** gave a linear relation in the Arrhenius plot in this temperature range (Figure 2b). It is assumed that the ImH_2^+ ions in **1″** are not well ordered as in **1**. The conductivity increases linearly and reaches 2.0×10^{-4} S cm^{-1} at 130 °C, which is slightly lower than for **1**, and the activation energy is 0.60 eV. We could not measure the conductivity of **1′** precisely because it was a transparent sticky solid; however, the unique mechanical flexibility of **1′** is promising for morphology control of the electrolyte in the fabrication of electrochemical devices, such as optimization of the electrode−electrolyte interface.

In conclusion, we have synthesized a new class of ionic plastic crystal by use of an extended coordination network and demonstrated its anhydrous proton conductivity. $[Zn(HPO_4)(H_2PO_4)_2](ImH_2)_2$ (**1**) consists of negatively charged 1D phosphate chains and positively charged ImH_2^+ ions, and it shows a proton conductivity of 2.5×10^{-4} S cm^{-1} at 130 °C. The conductivity increases nonlinearly at around 55 °C, which is attributed to an acceleration of motion of the involved ImH_2^+, as studied by XRD, DSC, and solid-state NMR spectroscopy. Through the plastic phase, **1** melts at 160 °C and changes to an amorphous solid **1′**. **1′** recrystallizes to give **1″**, which has a structure similar to that of **1** with long-range order but short-range disorder. The result suggests a method of construction of ionic plastic crystals by a variety of coordination networks and countercations/anions. Possible practical advantages of CIPCs compared with the conventional discrete ionic plastic crystals are the negligible volume change upon phase transformation, water durability, and wide temperature range of the plastic phase with a small entropy of fusion. Intense developments of coordination framework chemistry with internal spaces[8] would contribute to the area of plastic crystal and solid ion-conducting materials.

■ ASSOCIATED CONTENT

Ⓢ Supporting Information

Sample preparation; IR, TGA, and XRD data; solid-state ^{31}P and ^{2}H NMR spectra; and DSC and OCV measurements. This material is available free of charge via the Internet at http://pubs.acs.org.

■ AUTHOR INFORMATION

Corresponding Author

horike@sbchem.kyoto-u.ac.jp; kitagawa@icems.kyoto-u.ac.jp

Notes

The authors declare no competing financial interest.

■ ACKNOWLEDGMENTS

This work was supported by the Japan Science and Technology Agency PRESTO Program, Grants-in-Aid for Scientific Research, the Japan Society for the Promotion of Science

(JSPS), and the Japan Science and Technology Agency ERATO Program. iCeMS is supported by the World Premier International Research Initiative (WPI), MEXT, Japan.

REFERENCES

(1) (a) Timmermans, J. *J. Phys. Chem. Solids* **1961**, *18*, 1. (b) Sherwood, J. N. *The Plastically Crystalline State: Orientationally Disordered Crystals*; Wiley: Chichester, U.K., 1979. (c) MacFarlane, D. R.; Forsyth, M. *Adv. Mater.* **2001**, *13*, 957. (d) Haile, S. M.; Boysen, D. A.; Chisholm, C. R. I.; Merle, R. B. *Nature* **2001**, *410*, 910. (e) Pringle, J. M.; Howlett, P. C.; MacFarlane, D. R.; Forsyth, M. *J. Mater. Chem.* **2010**, *20*, 2056.

(2) (a) Cooper, E. I.; Angell, C. A. *Solid State Ionics* **1986**, *18−19*, 570. (b) Alarco, P. J.; Abu-Lebdeh, Y.; Abouimrane, A.; Armand, M. *Nat. Mater.* **2004**, *3*, 476. (c) Yoshizawa-Fujita, M.; Fujita, K.; Forsyth, M.; MacFarlane, D. R. *Electrochem. Commun.* **2007**, *9*, 1202. (d) Rana, U. A.; Bayley, P. M.; Vijayaraghavan, R.; Howlett, P.; MacFarlane, D. R.; Forsyth, M. *Phys. Chem. Chem. Phys.* **2010**, *12*, 11291.

(3) (a) Stallmach, F.; Groger, S.; Kunzel, V.; Karger, J.; Yaghi, O. M.; Hesse, M.; Muller, U. *Angew. Chem., Int. Ed.* **2006**, *45*, 2123. (b) Uemura, T.; Horike, S.; Kitagawa, K.; Mizuno, M.; Endo, K.; Bracco, S.; Comotti, A.; Sozzani, P.; Nagaoka, M.; Kitagawa, S. *J. Am. Chem. Soc.* **2008**, *130*, 6781.

(4) (a) Bureekaew, S.; Horike, S.; Higuchi, M.; Mizuno, M.; Kawamura, T.; Tanaka, D.; Yanai, N.; Kitagawa, S. *Nat. Mater.* **2009**, *8*, 831. (b) Hurd, J. A.; Vaidhyanathan, R.; Thangadurai, V.; Ratcliffe, C. I.; Moudrakovski, I. L.; Shimizu, G. K. H. *Nat. Chem.* **2009**, *1*, 705. (c) Umeyama, D.; Horike, S.; Inukai, M.; Hijikata, Y.; Kitagawa, S. *Angew. Chem., Int. Ed.* **2011**, *50*, 11706.

(5) (a) Li, Q. F.; He, R. H.; Jensen, J. O.; Bjerrum, N. J. *Chem. Mater.* **2003**, *15*, 4896. (b) Schuster, M. E.; Meyer, W. H. *Annu. Rev. Mater. Res.* **2003**, *33*, 233. (c) Laberty-Robert, C.; Valle, K.; Pereira, F.; Sanchez, C. *Chem. Soc. Rev.* **2011**, *40*, 961. (d) Tezuka, T.; Tadanaga, K.; Hayashi, A.; Tatsumisago, M. *J. Am. Chem. Soc.* **2006**, *128*, 16470. (e) Jin, Y. C.; Shen, Y. B.; Hibino, T. *J. Mater. Chem.* **2010**, *20*, 6214.

(6) (a) Chippindale, A. M.; Brech, S. J.; Cowley, A. R.; Simpson, W. M. *Chem. Mater.* **1996**, *8*, 2259. (b) Natarajan, S.; Neeraj, S.; Rao, C. N. R. *Solid State Sci.* **2000**, *2*, 87. (c) Liu, W.; Chen, H. H.; Yang, X. X.; Li, M. R.; Ge, M. H.; Zhao, J. T. *Chem. Lett.* **2004**, *33*, 1282. (d) Duan, F. Z.; Li, J. Y.; Chen, P.; Yu, J. H.; Xu, R. R. *Microporous Mesoporous Mater.* **2009**, *126*, 26.

(7) Kreuer, K. D. *Chem. Mater.* **1996**, *8*, 610.

(8) (a) Yaghi, O. M.; Li, H. L.; Davis, C.; Richardson, D.; Groy, T. L. *Acc. Chem. Res.* **1998**, *31*, 474. (b) Kitagawa, S.; Kitaura, R.; Noro, S. *Angew. Chem., Int. Ed.* **2004**, *43*, 2334. (c) Férey, G. *Chem. Soc. Rev.* **2008**, *37*, 191. (d) Shimizu, G. K. H.; Vaidhyanathan, R.; Taylor, J. M. *Chem. Soc. Rev.* **2009**, *38*, 1430. (e) Hupp, J. T.; Farha, O. K. *Acc. Chem. Res.* **2010**, *43*, 1166. (f) Yuan, D. Q.; Zhao, D.; Sun, D. F.; Zhou, H. C. *Angew. Chem., Int. Ed.* **2010**, *49*, 5357. (g) Shustova, N. B.; McCarthy, B. D.; Dincă, M. *J. Am. Chem. Soc.* **2011**, *133*, 20126. (h) Wiers, B. M.; Foo, M. L.; Balsara, N. P.; Long, J. R. *J. Am. Chem. Soc.* **2011**, *133*, 14522.